Role of SARS-CoV-2 nucleocapsid protein in affecting immune cells and insights on its molecular mechanisms

YAN LU[1], ZIYU YE[1], XINLAN LIU[2], LIQIAN ZHOU[1], XIANG DING[2] and YILING HOU[1]

[1]Key Laboratory of Southwest China Wildlife Resources Conservation (Ministry of Education), College of Life Sciences; [2]Key Laboratory of Nanchong City of Ecological Environment Protection and Pollution Prevention in Jialing River Basin, College of Environmental Science and Engineering, China West Normal University, Nanchong, Sichuan 637009, P.R. China

Received February 10, 2023; Accepted August 7, 2023

DOI: 10.3892/etm.2023.12203

Abstract. The present study aimed to explore the immune regulatory function of severe acute respiratory syndrome coronavirus 2 (SARS-CoV-2) nucleocapsid (N) protein and related mechanisms. In a series of protein activity experiments, SARS-CoV-2 N protein promoted proliferation of three immune cell lines: mouse Raw264.7, human Jurkat and human Raji in a dose-dependent manner. A total of 10 μg/ml N protein could significantly change cell cycle progression of the aforementioned three immune cell lines and could promote quick entry of Raw264.7 cells into G_2/M phase from S phase to achieve rapid growth. Additionally, the N protein could also stimulate Raw264.7 cells to secrete a number of proinflammatory factors such as TNF-α, IL-6 and IL-10. RNA sequencing analysis indicated that the N protein changed the expression of certain genes involved in immune-related functions and four important signaling pathways, including JAK-STAT, TNF, NF-κB and MAPK signaling pathways, which suggested that the N protein may not only regulate the expression of genes involved in the process of resisting viral infection in macrophages of the immune system, but also change cellular signal processing.

Correspondence to: Professor Xiang Ding, Key Laboratory of Nanchong City of Ecological Environment Protection and Pollution Prevention in Jialing River Basin, College of Environmental Science and Engineering, China West Normal University, 1 Shida Road, Nanchong, Sichuan 637009, P.R. China
E-mail: biostart8083@126.com

Professor Yiling Hou, Key Laboratory of Southwest China Wildlife Resources Conservation (Ministry of Education), College of Life Sciences, China West Normal University, 1 Shida Road, Nanchong, Sichuan 637009, P.R. China
E-mail: starthlh@126.com

Key words: severe acute respiratory syndrome coronavirus 2 nucleocapsid, immune cells, cell cycle, differently expressed genes, signaling pathway

Introduction

By the end of 2019, a new coronavirus strain was identified as the cause of the coronavirus disease 2019 (COVID-19), which swept the globe and posed a threat to public health because infection with this coronavirus causes severe inflammatory responses (1,2). The virus was named severe acute respiratory syndrome coronavirus 2 (SARS CoV-2) on February 11 2020 by the International Committee on Taxonomy of Viruses (3). SARS-CoV-2 is an enveloped virus with a single-stranded, positive-sense RNA genome belonging to the β-coronavirus subfamily of *Coronaviridae* (4-6). The genome size of SARS-CoV-2 is 29,903 nucleotides-long, encoding 16 non-structural proteins, 9 accessory proteins and 4 structural proteins, including spike (S), envelope, membrane (M) and nucleocapsid (N) proteins (7). Among them, the N protein is one of the most important structural proteins; it is highly conversed and its fundamental function is to package viral RNA into ribonucleocapsid particles, and it interacts with the M protein in viral assembly (6-9).

In addition, several previous studies show that the N protein of SARS-CoV-2 could also be involved in the regulation of processes of the host immune response (10-12). The immune response to viral infection includes the innate immune response that ensues immediately after infection as well as adaptive immunity, which comes after a delay of 4-5 days (13). In innate immunity, RNA interference (RNAi) is recognized as a cell-intrinsic antiviral immune process in numerous eukaryotes, including mammals (14). A previous study showed that the SARS-CoV-2 N protein could act in multiple steps against RNAi through RNA-binding activities (10). Moreover, the production of IFN is considered the hallmark of antiviral response induced by innate immunity (15). Studies showed that the N protein is a potent IFN antagonist, not only by targeting the retinoic acid inducible gene I (11), but also by suppressing the expression of IFN-stimulated genes through inhibiting the phosphorylation and nuclear translocation of STAT1/STAT2 (12). The result from these previous studies indicated that the SARS-CoV-2 N protein may lead to the exacerbation of innate immune responses and to increased inflammation.

Although there has been some notable research on the SARS-CoV-2 N protein, further investigation is required, including the ability of the N protein to regulate immunity

and its mechanisms. The present study aimed to explore the effect of the N protein on the activity of three types of immune cells *in vitro*, including Raw264.7, a mouse leukemia macrophage cell line that mainly serves a role in the innate immune response and also stimulates lymphocytes and other immune cells in response to pathogens, Jurkat, a human lymphoblastic leukemia T lymphocyte cell line, and Raji, a human Burkitt lymphoma B lymphocyte cell line; T and B lymphocytes mainly participate in the adaptive immune response. In addition, the current study aimed to provide a theoretical basis for the molecular mechanism by which the N protein influences host immunity by investigating the key signaling pathways or molecules using RNA sequencing.

Materials and methods

Escherichia coli expression strain of the N protein. The *E. coli* expression strain of the N protein of SARS-CoV-2 was donated by the Guangdong Laboratory Animals Monitoring Institute (Guangzhou, China).

Cell lines and culture. Raw264.7 (mouse macrophages), Jurkat (human T lymphocytes) and Raji (human B lymphocytes) cell lines were purchased from the Center for Excellence in Molecular Cell Science (Shanghai, China). Cells were cultured in RPMI-1640 (Gibco; Thermo Fisher Scientific, Inc.) with the addition of 10% FBS (Gibco; Thermo Fisher Scientific, Inc.), 100 U/ml penicillin and 100 μg/ml streptomycin sulfate (Gibco; Thermo Fisher Scientific, Inc.) in a humidified incubator with 5% CO_2 at 37˚C.

Reagents. Cell Counting Kit-8 (CCK-8) was purchased from Dojindo Laboratories, Inc. The Cell Cycle and Apoptosis Analysis (cat. no. C1052) and His-tag Protein Purification Kit (denaturation-resistant; cat. no. P2210) were purchased from Beyotime Institute of Biotechnology. Lipopolysaccharide (LPS) and concanavalin A (ConA) were purchased from Sigma-Aldrich (Merck KGaA). PageRuler™ Prestained protein ladder (cat. no. 26616) was purchased from Thermo Fisher Scientific, Inc. Trypsin-EDTA (0.25%) used to digest Raw264.7 cells for cell passage was purchased from Gibco; Thermo Fisher Scientific Inc. TNF-α Elisa kit (Cat. no. EK0527), IL-6 Elisa Kit (Cat. no. EK0411), IL-10 Elisa Kit (Cat. no. EK0417) and CD163 ELISA kit (Cat. no. EK1146) were purchased from Boster Biological Technology co., Ltd.).

Expression and purification of the N protein of SARS-CoV-2. The *E. coli* expression strain of the SARS-CoV-2 N protein was grown in Luria-Bertani medium with 50 μg/ml kanamycin at 37˚C for 2.5-3.0 h with shaking speed at 220 rpm until the optical density (OD) 600 nm reached 0.6-0.8. The cells were subsequently induced with 0.5 mM isopropyl β-D-1-thiogalactopyranoside for 16-20 h at 16˚C with shaking speed at 220 rpm. The induced *E. coli* cells were harvested by centrifugation at 8,000 x g for 30 min at 4˚C and stored at -80˚C. Purification of the N protein was performed following the mass purification of His-tag protein under non-denaturing conditions according manufacturer's instructions. The eluted N protein was added into a dialysis bag [molecular weight (MW), 7 kDa] into 2 l dialysis buffer, stirred at 4˚C for ~6 h with the dialysis buffer replaced every 2 h. Protein samples were filtered and sterilized using 0.22 μm needle hole filter. After the protein concentration was determined using a UV spectrophotometer (Nova2000; Thermo Fisher Scientific, Inc.), the N protein was analyzed by SDS-PAGE (10% SDS-PAGE, 2 μg/well, detection of protein bands by Coomassie brilliant blue R250 staining for 2-4 h at room Temperature), sub-packaged (divide the filtered and sterilized N protein into sterile 2 ml protein storage tubes, 1 ml/tube) and stored at -80˚C. The Spectra™ Multicolor High Range Protein Ladder (cat. no. 26625; Thermo Fisher Scientific, Inc.) was used as the protein MW standard. During the induction and purification processes, the induced and uninduced lysis supernatants, the N proteins eluted of different elution times, and the flow through fluid of different elution times were used as controls for SDS-PAGE. The results were analysed using Image Lab 6.0 (Bio-Rad Laboratories, Inc.).

Cell viability assay. Cell viability was measured by CCK-8 according to the manufacturer's instructions. Raw264.7, Jurkat and Raji cells were cultured at a density of $8x10^3$ cells/well in 100 μl medium in 96-well microplates with 5% CO_2 at 37˚C. The cells were treated with different concentrations of N protein (0, 0.3125, 1.25, 5, 10, 20 or 40 μg/ml) or with LPS (or ConA), used as positive control, at a final concentration of 10 μg/ml for 48 h. Then, 10 μl of CCK-8 reagent was added to the wells, and cells were cultured for 2-6 h at 37˚C to reach the optimum color development time. All experiments were performed in quintuplicate. The absorbance data were collected at 450 nm using a microplate reader. The viability of these cells treated with N protein was expressed as the absorbance.

Cell cycle assay. The cell cycle status was examined using the Cell Cycle and Apoptosis Analysis Kit according to the manufacturer's protocols. Raw264.7, Jurkat and Raji cells ($4x10^5$ cells/well) were grown in culture medium on six-well plates at 37˚C for 12 h. Next, cells were treated with either 0 or 10 μg/ml N protein, or with 10 μg/ml LPS at 37 ˚C for 24 h. After treatment, cells were harvested, washed with cold PBS and fixed in 70% ethanol at 4˚C for 12-24 h. Fixed cells were harvested, washed three times with cold PBS, centrifuged at 1,000 x g for 5 min at 4˚C, resuspended in 500 μl propidium iodide dye buffer and incubated for 30 min at 37˚C in the dark. Cells were stored in the dark at 4˚C or in an ice bath. The DNA content of the collected 20,000 cells was detected by flow cytometry within 24 h. The percentage of cells in G_0/G_1, S and G_2/M phases was then analyzed using FlowJo V10 (BD Biosciences).

Quantification of TNF-α, IL-6, IL-10 and CD163 of treated Raw264.7 cells. Raw264.7 cells ($4x10^5$ cells/well) were cultured in six-well plates. After 12 h-starvation at 37˚C with 5% CO_2, cells were treated with either 0 or 10 μg/ml N protein, or with 10 μg/ml ConA for 48 h. The culture medium obtained from the treated Raw264.7 cells was centrifuged at 600 x g for 10 min at 4˚C and the supernatant was collected. Concentrations of TNF-α, IL-6, IL-10 and CD163 in the cultured supernatant were measured using a mouse ELISA kit (Boster Biological Technology Co., Ltd.) according to the manufacturer's instructions.

Transcriptome analysis of Raw264.7 Cell. Raw264.7 cells were planted in 75-cm^2 cell culture tanks and treated with 10 μg/ml N protein or 10 μg/ml ConA, used as positive control, at 37˚C for 24 h. Untreated cells were used as blank control; experiments were repeated three times. After incubation, cells were harvested, washed once with cold PBS and transferred into 1.5-ml Eppendorf tubes. It was ensured that all the pipette tips and tubes did not contain any RNase or DNase. After washing, the tubes of the harvested cells were snap frozen in liquid nitrogen and transported with dry ice to Novogene Co., Ltd. for RNA extraction, cDNA library construction and sequencing. Total RNA was extracted using TRIzol™ (Invitrogen; Thermo Fisher Scientific, Inc.). RNA integrity and quantity were assessed using the RNA Nano 6000 Assay Kit of the Bioanalyzer 2100 system (Agilent Technologies, Inc.). The cDNA library was constructed, and the library quality was assessed on the Agilent Bioanalyzer 2100 system. After the cDNA library was qualified, sequencing was performed using the Illumina NovaSeq 6000 (Illumina, Inc.), S4 suite components.

The clean reads were obtained by removing reads containing adapter, poly-N and low-quality reads from raw data. All downstream analyses were based on the clean data. Reference genome (ftp.ensembl.org/pub/release-104/fasta/mus_musculus/) and gene model annotation files (ftp.ensembl.org/pub/release-104/gtf/mus_musculus/) were downloaded from genome website directly. Clean reads were mapped to the reference genome using Hisat2 (version 2.0.5; daehwankimlab.github.io/hisat2/. Quantification of gene expression was carried using featureCounts (version 1.5.0-p3) to count the reads numbers mapped to each gene (subread.sourceforge.net/. Fragments per kilobase of transcript per million mapped reads (FPKM) of each gene was calculated based on the length of the gene and read count mapped to this gene. Differential expression analysis of two groups was performed using DESeq2 R package (version 1.20.0; github.com/thelovelab/DESeq2. Benjamini and Hochberg's method was used to adjust the P-value for controlling the false discovery rate. Genes with an adjusted P-value (P_{adj})<0.05 and $|\log_2 FC|>1$ were set as the threshold for significant differential expression. Gene Ontology (GO) enrichment analysis of differentially expressed genes (DEGs) was implemented by the cluster Profiler R package (version 3.8.1), in which gene length biases were corrected. GO terms with $P_{adj} \leq 0.05$ were considered significantly. Cluster profiler R package was used to test the statistical enrichment of DEGs in Kyoto Encyclopedia of Genes and Genomes (KEGG) pathways.

Statistical analysis. Statistical analysis was performed using IBM SPSS Statistics 23 (IBM Corp.), and all the quantitative data were presented as the mean ± SD. A one-way analysis of variance followed by Tukey's post hoc test was used to compare data among groups when they had a normal distribution and homogeneous variances. P<0.05 was considered to indicate a statistically significant difference.

Results

Purification of N protein of SARS-CoV-2. SDS-PAGE analysis revealed that the main band with MW ~47 kDa was the purified N protein of SARS-CoV-2 (Fig. 1). The purity of the products was >92% estimated by analysis using Image Lab 6.0 (Bio-Rad Laboratories, Inc.).

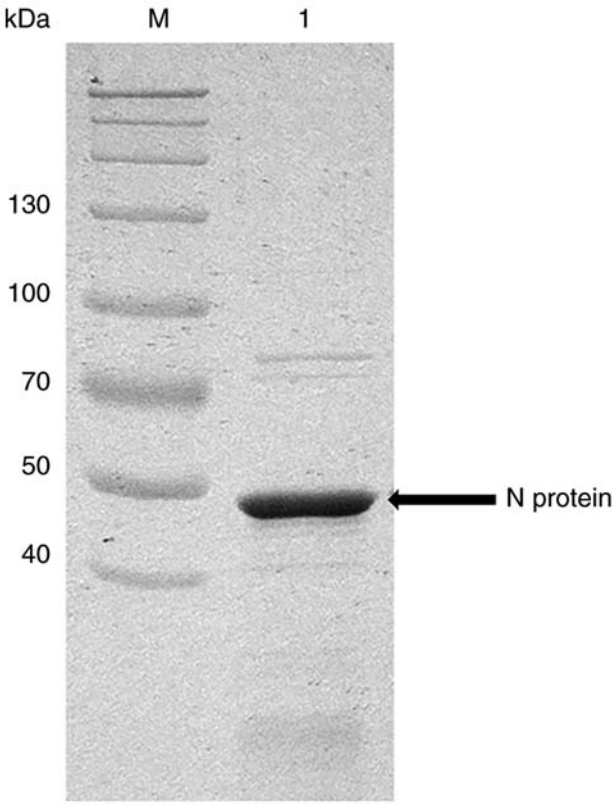

Figure 1. Analysis of purification of the SARS-CoV-2 N protein by 10% SDS-PAGE. Lane M, Spectra Multicolor High Range Protein Ladder; lane 1, purified N protein of SARS-CoV-2. N, nucleocapsid protein; SARS-CoV-2, severe acute respiratory syndrome coronavirus 2.

Cell viability. The CCK-8 assay was used to determine the effects of treatment with different concentrations of N protein for 48 h on the viability of Raw264.7, Jurkat and Raji cells. As shown in Fig. 2A-C, the OD_{450} of the viability of Raw264.7 cells treated with N protein at ≥1.25 μg/ml was significantly higher than that of the control group (P<0.01), displaying a dose-dependent trend. In Jurkat and Raji cells, this effect appeared at ≥1.25 μg/ml. It was concluded that the N protein of SARS-CoV-2 could stimulate the viability of Raw264.7, Jurkat and Raji cells in a dose-dependent manner. It is worth noting that when the concentration of the N protein was either 10, 20 or 40 μg/ml, the viability of Raw264.7 cells increased by 66.98, 87.72 and 99.29% respectively; the viability of Jurkat cells increased by 104.30, 122.05 and 123.94% respectively; and the viability of Raji cells was increased by 110.67, 141.03 and 154.38%, respectively. Morphological changes of these cells (Raw264.7 cells adhered to the wall and grew, with some cells extending pseudopodia, Jurkat cells and Raji cells grow larger and clumped) were also noted following N protein treatment (Fig. 2D-F). Based on the aforementioned results, the concentration of 10 μg/ml N protein was selected for subsequent experiments.

Cell cycle analysis. The effects of N protein on cell cycle distribution were detected by flow cytometry to analyze cellular DNA content. After 24-h treatment with

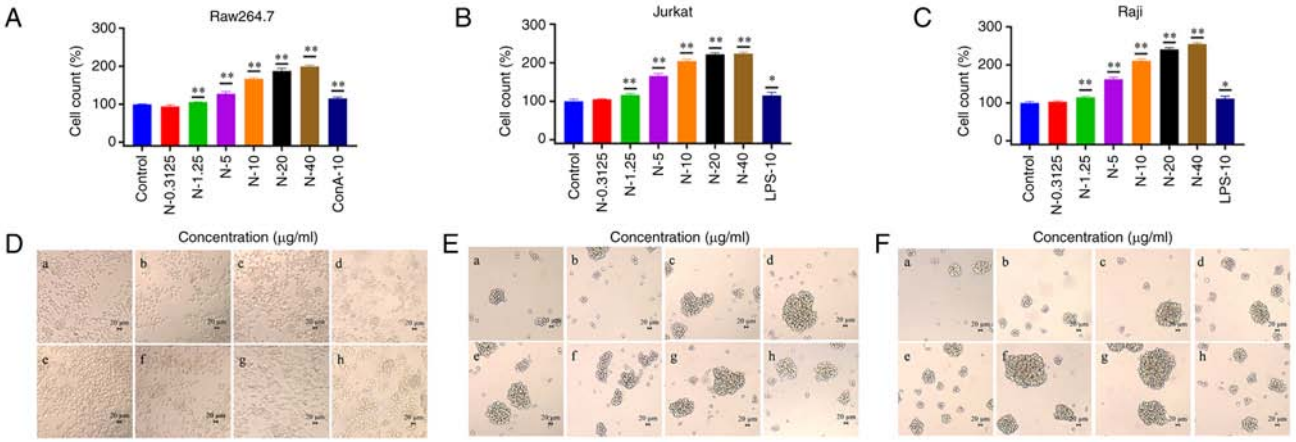

Figure 2. Viability effects of different doses of severe acute respiratory syndrome coronavirus 2 N protein on three cell lines. Effects of N protein on the viability of (A) Raw264.7, (B) Jurkat and (C) Raji cells. Cell morphology observations in (D) Raw264.7, (E) Jurkat and (F) Raji cells. (a) Control group; (b) 0.3125 μg/ml N protein; (c) 1.25 μg/ml N protein; (d) 5 μg/ml N protein; (e) 10 μg/ml N protein; (f) 20 μg/ml N protein; (g) 40 μg/ml N-protein; (h) positive group, 10 μg/ml ConA in Raw264.7 cells or 10 μg/ml LPS in Jurkat and Raji cells. Data are presented as mean ± SD (n=5). *P<0.05 and **P<0.01 vs. blank control. ConA, concanavalin A; LPS, lipopolysaccharide; N, nucleocapsid protein; OD450, optical density values at 450 nm.

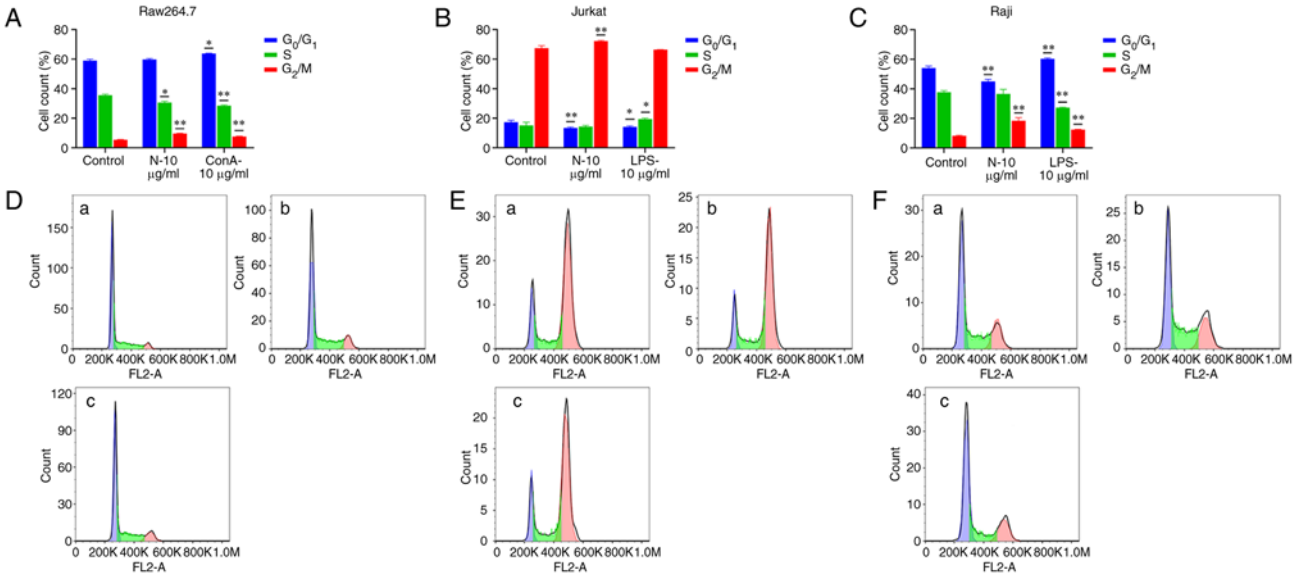

Figure 3. Cell cycle analysis following treatment with the severe acute respiratory syndrome coronavirus 2 N protein. Results of cell cycle analysis in (A) Raw264.7, (B) Jurkat and (C) Raji cells. Representative flow cytometry plots of (D) Raw264.7, (E) Jurkat and (F) Raji cells. (a) Control group; (b) 10 μg/ml N protein; (c) positive group, 10 μg/ml ConA in Raw264.7 cells or 10 μg/ml LPS in Jurkat and Raji cells. Data are presented as mean ± SD. *P<0.05 and **P<0.01 vs. blank control. ConA, concanavalin A; LPS, lipopolysaccharide; N, nucleocapsid protein.

10 μg/ml N protein, the percentage of Raji and Jurkat cells in the G_0/G_1 phase significantly decreased, and that of cells in the G_2/M phase significantly increased compared with the respective control (P<0.01; Fig. 3B, C, E and F). In Raw264.7 cells, there was a significant increase in the percentage of cells in the G_2/M phase compared with the control (P<0.01; Fig. 3A and D). By contrast, there was no significant change in the percentage of cells in the G_0/G_1 phase, and a significant decrease was observed in the percentage of cells in the S phase (P<0.05). These data indicated that 10 μg/ml N protein significantly changed the cell cycle progression of the three immune cell lines and may promote the rapid entry of Raw264.7 cells into the G_2/M phase from the S phase, potentially leading to increased cell proliferation.

Quantification of TNF-α, IL-6, IL-10 and CD163. The levels of TNF-α, IL-10, IL-6 and CD163 were determined in the supernatant of cultured Raw264.7 cells in the control group, N protein group (10 μg/ml) and ConA group (10 μg/ml) (Fig. 4A-D). The SARS-Cov-2 N protein stimulated Raw264.7 cells to secrete TNF-α, IL-10, IL-6, but not CD163. This suggested that the N protein may promote macrophages to secrete proinflammatory factors.

Cell transcriptome analysis. Based on the results of the cell viability and cell cycle assays, the concentration of 10 μg/ml N protein and the Raw264.7 cell line were chosen to analyze the cell transcriptome for further exploration of the molecular mechanism of the N protein affecting the immune system. An average of 6.60, 6.61 and 6.84 Gb raw data were obtained

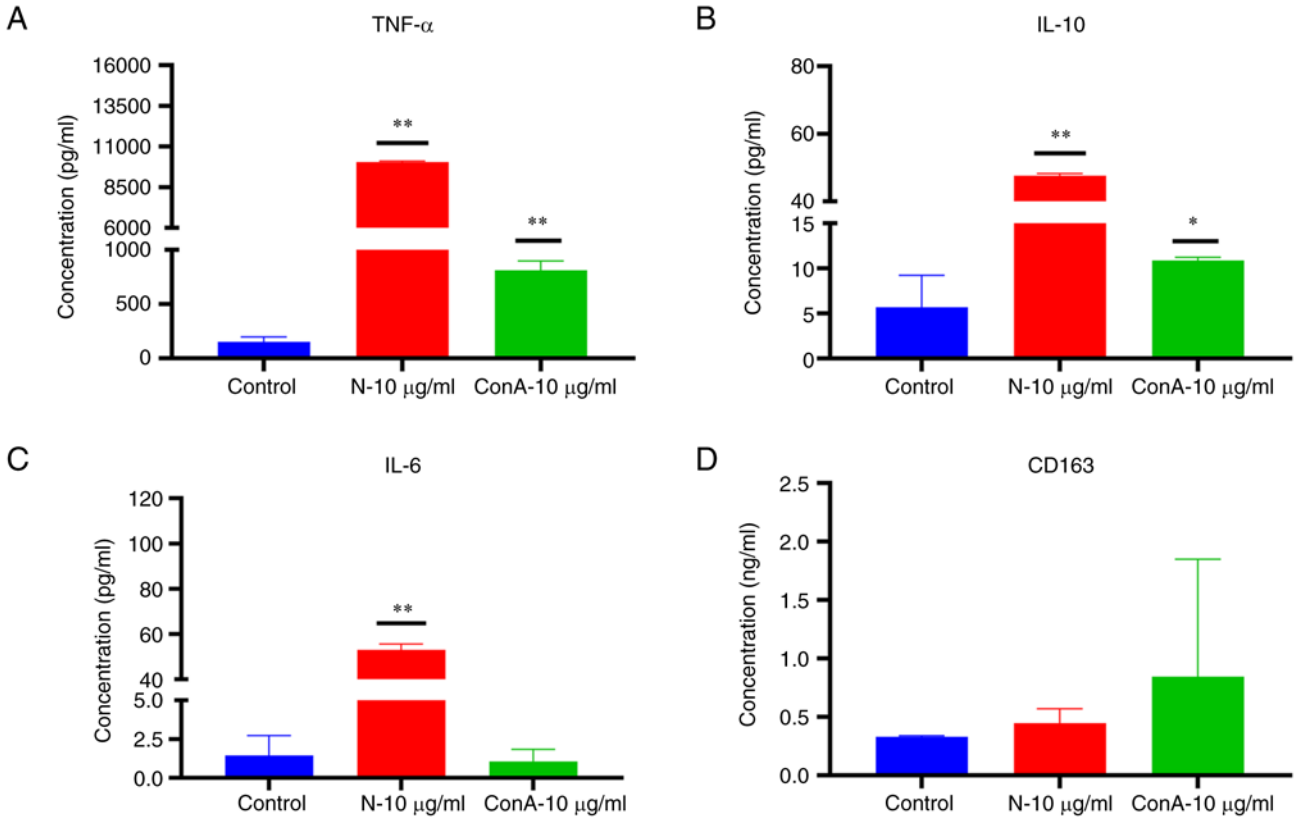

Figure 4. Quantification of TNF-α, IL-10, IL-6 and CD163. The concentrations of (A) TNF-α, (B) IL-10, (C) IL-6 and (D) CD163 were determined in the supernatant of cultured Raw264.7 cells treated with the severe acute respiratory syndrome coronavirus 2 N protein. Data are presented as mean ± SD (n=3). *P<0.05 and **P<0.01 vs. blank control.

from the libraries of the control, ConA and N protein groups, respectively. After filtering, clean data (accuracy rate, 98.18, 95.31 and 94.44%, respectively for the aforementioned three groups) were used for subsequent analysis. The quality (Q)20 and Q30 of the samples were ≥95.8 and ≥89%, respectively. The GC content range of all samples was 47.96-50.81%. These results indicated that the sequencing results were of high reliability.

Quantification of the gene expression level. Genes of FPKM >0.3 were considered expressed, and those of FPKM >60 were considered highly expressed. Results showed that a total of 13,899 genes (24.94%) were expressed in the control group, with 930 genes (1.67%) expressed at high levels. A total of 13,551 genes (24.32%) were expressed in the ConA group with 995 genes (1.79%) expressed at high levels, and a total of 13,610 genes (24.43%) were expressed in the N group with 861 genes (1.54%) expressed at high levels.

Further analysis revealed that: i) Seven genes, including *mt-Co1, Lyz2, Eef1a1, mt-Cytb, Rplp1, Rn18s* and *mt-Nd*, were expressed at high levels in the control group (Table I); ii) eight genes, *mt-Co1, Lyz2, Eef1a1, Rplp1, mt-Cytb, Spp1, mt-Nd1* and *Ftl1*, were expressed at high levels in the ConA group (Table II); and iii) five genes, *mt-Co1, Eef1a1, Lyz2, Rplp1* and *Spp1*, were expressed at high levels in the N group (Table III). *mt-Co1*, *mt-Cytb* and *mt-Nd1* encode part of three different multisubunit complexes located in the inner mitochondrial membrane, which are important in high-energy electron transfer of respiratory chain (16-18). *mt-Co1* was expressed at high levels in all three groups, and its FPKM was 8,636.39, 6,619.55 and 4,300.42 in the control, ConA and N group, respectively, whereas *mt-Cytb* and *mt-Nd1* were not expressed at high levels in the N group. These results suggested that treatment with the N protein, but not with ConA, may decrease energy-conversion processes to generate ATP during oxidative phosphorylation of Raw264.7 cells. *Spp1* encodes the secretory phosphoprotein 1 (19), which was expressed at high levels in the N and ConA groups with FPKM 2,253.54 and 2,898.29, respectively. This suggested that the N protein may stimulate Raw264.7 cells to secrete cytokines, functionally similar to ConA.

Differential expression analysis and functional enrichment of DEGs. To identify the significant DEGs (P_{adj} <0.05; $|\log_2 FC|$ >1), the FPKM was compared. As shown in Fig. 5A and B, 21,279 genes were significantly differentially expressed in the ConA compared with those in the control group; of these, 177 genes were upregulated and 293 downregulated. The top ten DEGs of log2|FC| are shown in Table IV. In addition, 20,349 genes were significantly differentially expressed in the N protein group compared with the control group, with 626 genes upregulated and 980 downregulated. The top ten DEGs of $\log_2 FC$ are shown in Table V.

To comprehensively understand the roles of these DEGs, GO term enrichment analysis was conducted. In the ConA group, compared with the control group, the upregulated DEGs were significantly enriched in GO biological processes (BP) terms 'lymphocyte migration' and 'lymphocyte chemotaxes', in GO

Table I. Quantification of gene expression in the control group (FPKM >2,000).

Gene	Description	FPKM	Length, bp
mt-Co1	Mitochondrially encoded cytochrome *c* oxidase I	8,636.39	1,545
Lyz2	Lysozyme 2	6,868.05	1,316
Eef1a1	Eukaryotic translation elongation factor 1 α 1	5,144.65	2,493
mt-Cytb	Mitochondrially encoded cytochrome *b*	3,703.39	1,144
Rplp1	Ribosomal protein, large, P1	2,840.85	499
Rn18s	18S ribosomal RNA	2,680.08	1,849
mt-Nd1	Mitochondrially encoded NADH dehydrogenase 1	2,657.22	957

FPKM, fragments per kilobase of transcript per million mapped reads.

Table II. Quantification of gene expression in the concanavalin A group (FPKM >2,000).

Gene	Description	FPKM	Length, bp
mt-Co1	Mitochondrially encoded cytochrome *c* oxidase I	6,619.55	1,545
Lyz2	Lysozyme 2	6,467.67	1,316
Eef1a1	Eukaryotic translation elongation factor 1 α 1	4,945.56	2,493
Rplp1	Mitochondrially encoded cytochrome *b*	3,726.39	499
mt-Cytb	Ribosomal protein, large, P1	3,328.82	1,144
Spp1	18S ribosomal RNA	2,898.29	1,648
mt-Nd1	Mitochondrially encoded NADH dehydrogenase 1	2,594.37	957
Ftl1	Ferritin light polypeptide 1	2,514.88	1,340

FPKM, fragments per kilobase of transcript per million mapped reads.

Table III. Quantification of gene expression in the nucleocapsid group (FPKM >2,000).

Gene	Description	FPKM	Length, bp
mt-Co1	Mitochondrially encoded cytochrome *c* oxidase I	4300.42	1,545
Eef1a1	Eukaryotic translation elongation factor 1 α 1	4239.39	2,493
Lyz2	Lysozyme 2	3791.70	1,316
Rplp1	Ribosomal protein, large, P1	3647.46	499
Spp1	Secreted phosphoprotein 1	2253.54	1,648

FPKM, fragments per kilobase of transcript per million mapped reads.

cellular component (CC) terms 'side of membrane' and 'actin cytoskeleton', and GO molecular function (MF) terms 'integrin binding' and 'cell adhesion molecule binding' (Fig. 5C). Downregulated DEGs were significantly enriched in GO BP terms 'regulation of leukocyte activation' and 'positive regulation of immune response', in GO CC terms 'external side of plasma membrane' and 'side of membrane', and in GO MF terms 'cytokine receptor binding' and 'cytokine activity'(Fig. 5D). Compared with the control, the DEGs of the N protein group were quite different from those of ConA group (Fig. 5E and F). Compared with the control group, the upregulated DEGs of the N protein group were significantly enriched in 56 GO terms, including five MF terms, such as 'double-stranded RNA binding' and 'adenylyltransferase activity', and 51 BP terms in which there were 15 terms associated with virus, such as 'response to virus' and 'defense response to virus', 14 terms associated with IFN such as 'response to interferon-beta'. Furthermore, downregulated DEGs were most significantly enriched in GO BP term the 'inflammatory response' and 'leukocyte cell-cell adhesion', and in GO MF terms 'protein tyrosine/threonine phosphatase activity' and 'MAP kinase tyrosine/serine/threonine phosphatase activity'. The aforementioned GO terms indicated that the SARS-CoV-2 N protein, rather than ConA, could not only regulate the expression of genes involved in resisting viral infection in macrophages of the immune system, but also change cellular signal processing.

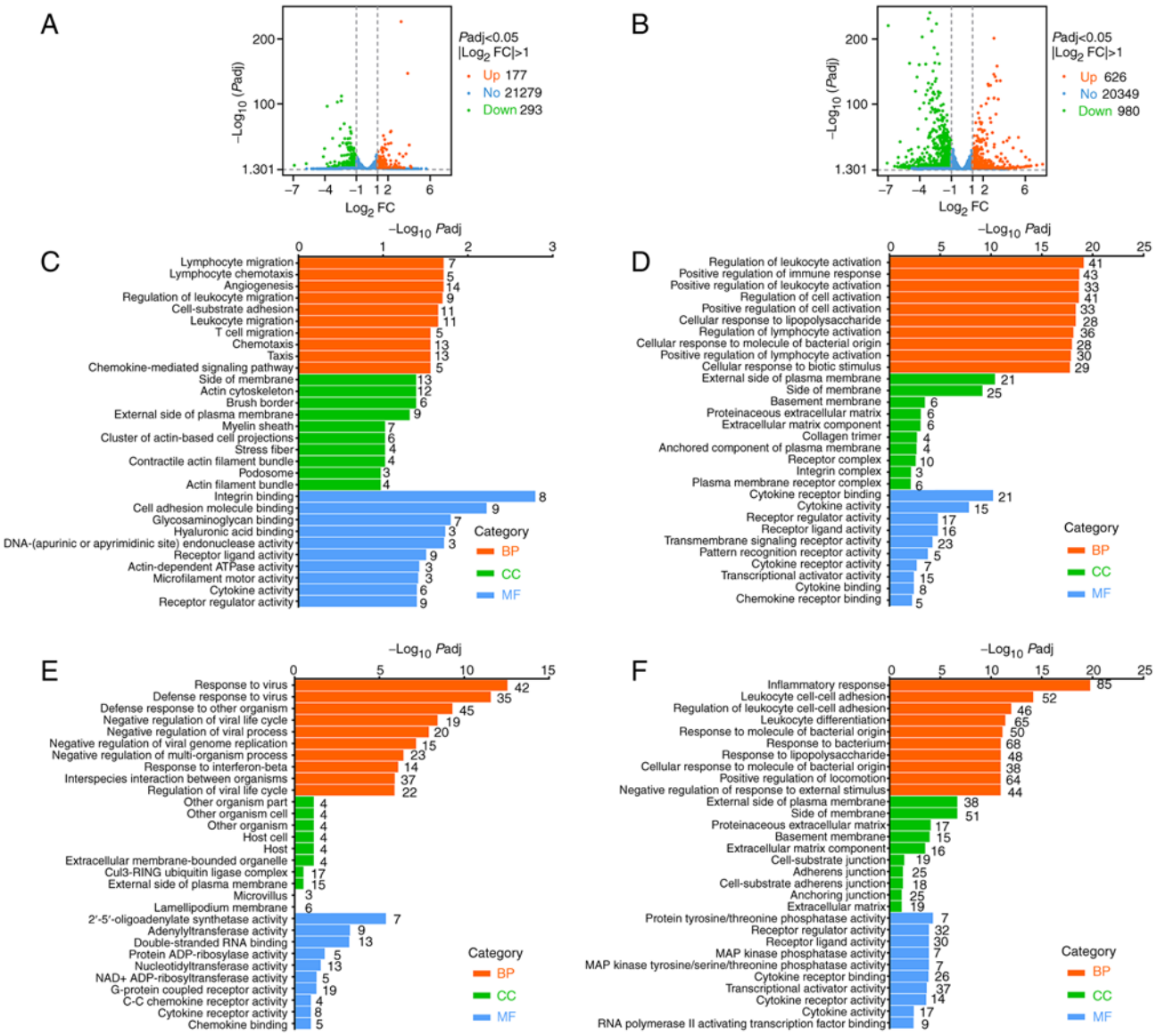

Figure 5. DEG analysis (A) Volcano plots showing expression level of each Gene in ConA group compared with the control group. (B) Volcano plots showing expression level of each UniGene in the N group compared with that of the control group. Limits defined by $P_{adj} \leq 0.05$ and $|\log_2 FC| > 1$. GO functional term classification of (C) upregulated and (D) downregulated DEGs of ConA group compared with the control group. GO functional classification of (E) upregulated and (F) downregulated DEGs of N protein group compared with the control group. BP, biological process; CC, cellular component; ConA, concanavalin A; DEGs, differentially expressed genes; GO, Gene Ontology; MF, molecular function; N, nucleocapsid protein.

KEGG pathway enrichment analysis. To better understand the interactions of the these DEGs, they were used in KEGG pathway enrichment analysis. The results showed that the upregulated DEGs of the ConA group were significantly enriched in five pathways compared with the control group, of which three are classified as 'metabolism' including 'carbon metabolism', 'glycolysis/gluconeogenesis' and 'biosynthesis of amino acids' (Fig. 6A). The downregulated DEGs were significantly enriched in 30 pathways with 17 being disease-related such as 'Prion diseases' and 'Pertussis', five associated with signal molecules and transduction such as 'TNF signaling pathway' and 'JAK-STAT signaling pathway', and eight classified as immune system such as 'C-type lection receptor signaling pathway' and 'hematopoietic cell lineage' (Fig. 6B). The upregulated DEGs of the N protein group compared with the control group were most significantly enriched in eight pathways including five disease-related ones such as 'Herpes simplex virus 1 infection' and 'Influenza A', and two classified as signaling molecules and interaction including 'TNF signaling pathway' and 'JAK-STAT signaling pathway', and the NOD-like receptor signaling pathway. The downregulated DEGs were most significantly enriched in 25 pathways of which 12 were disease-associated such as 'Staphylococcus aureus infection' and 'pathways in cancer', seven were related to signal molecules and transduction such as 'cytokine-cytokine receptor interaction' and 'TNF signaling pathway', and six were categorized as immune system such as 'complement and coagulation cascades' and 'C-type lectin receptor signaling pathway' (Fig. 6C and D). These results indicated that the N protein, similarly to ConA, could regulate the function of macrophages in the immune system from two

Table IV. DEGs of top ten log2FC in ConA group

Gene	Log2FC	Up/Down	Description
4833415N18Rik	4.20	Up	RIKEN cDNA 4833415N18 gene
Rgs16	4.14	Up	Regulator of G-protein signaling 16
Serpinb9b	4.01	Up	Serine (or cysteine) peptidase inhibitor, clade B, member 9b
Anpep	3.86	Up	Alanyl (membrane) aminopeptidase
Atp6v0d2	3.71	Up	ATPase, H+ transporting, lysosomal V0 subunit D2
Adgre4	-3.48	Down	Adhesion G protein-coupled receptor E4
Cdk5r1	-3.78	Down	Cyclin-dependent kinase 5, regulatory subunit 1 (p35)
Il1a	-4.03	Down	Interleukin 1 alpha
Il1b	-4.15	Down	Interleukin 1 beta
Csf3	-5.77	Down	Colony stimulating factor 3 (granulocyte)

Table V. The DEGs of top ten log2FC in N group

Gene	Log2FC	Up/Down	Description
Nos2	9.01	Up	Nitric oxide synthase 2, inducible
Ghr	7.63	Up	Growth hormone receptor
KlK9	7.07	Up	Kallikrein related-peptidase 9
Slc9b2	6.54	Up	Solute carrier family 9, subfamily B (NHA2, cation proton antiporter 2), member 2
Ptprn	6.41	Up	Protein tyrosine phosphatase, receptor type, N
Rgs16	6.39	Up	Regulator of G-protein signaling 16
Klk8	6.32	Up	Kallikrein related-peptidase 8
Selenop	-6.38	Down	Selenoprotein P
Ccrl2	-6.99	Down	Chemokine (C-C motif) receptor-like 2
Nr4a3	-7.09	Down	Nuclear receptor subfamily 4, group A, member 3

directions (up and down); that is, the N protein could not only upregulate the ability of macrophages to participate in innate immunity, but also downregulate their ability to participate in adaptive immunity. This suggested that after activating the innate immune response, N protein can down-regulate genes engaged in the differentiation of immune cells such as Th17 cell and antibody production such as intestinal immune network for IgA production in acquired immunity (shown in Fig. 6D). These data also suggested that the N protein may facilitate virus escape from the immune system as genes downregulated by N protein are significantly enriched in the acquired immune system, including Element and Coagulation Cascades, TH17 cell differentiation, Intrinsic immune network for IgA production, and Th1 and Th2 cell differentiation.

To explore the functional pathway involved in the N protein affecting Raw264.7 cells, the pathways that were categorized into signal transduction of KEGG enrichment analysis were examined in the N protein group compared with the control group. Results showed that there were four pathways including JAK-STAT, TNF, NF-κB and MAPK with $P_{adj}<0.05$ and $|\log_2FC|>1$ (Table VI). Key DEGs enriched were shown in Table VII. As in Table VII, the N protein could rise *Il12rb1* ($\log_2FC=1.13$; $P_{adj}=3.04x10^{-4}$) that may lead to JAK-STAT signaling cascade activation, then upregulate *STAT1* ($\log_2FC=1.09$; $P_{adj}=4.62x10^{-11}$) and *STAT2* ($\log_2FC=1.16$; $P_{adj}=5.67x10^{-13}$), which was in line with a previous study (13). Moreover, the N protein could significantly downregulate MPK-related genes of macrophages including *Dusp1* ($\log_2FC=-2.05$; $P_{adj}=3.2x10^{-118}$), *Dusp2* ($\log_2FC=-1.42$; $P_{adj}=4.04x10^{-5}$), *Dusp4* ($\log_2FC=-1.26$; $P_{adj}=8.76x10^{-28}$), *Dusp5* ($\log_2FC=-2.39$; $P_{adj}=5.81x10^{-110}$), *Dusp8* ($\log_2FC=-4.21$; $P_{adj}=8.22x10^{-16}$), *Dusp10* ($\log_2FC=-1.33$; $P_{adj}=1.08x10^{-4}$) and *Dusp16* ($\log_2FC=-1.68$; $P_{adj}=9.40x10^{-43}$), which was also previously reported by several studies (20,21). The present study showed that the N protein may downregulate *Cxcl1* ($\log_2FC=-5.89$; $P_{adj}=4.99x10^{-4}$), *Cxcl2* ($\log_2FC=-3.77$; $P_{adj}=4.38x10^{-204}$) and *Cxcl10* ($\log_2FC=-2.63$; $P_{adj}=1.54x10^{-40}$), which was inconsistent with a previous study (22). In addition, the present study also found that the N protein may not only downregulate *Malt1* ($\log_2FC=-2.25$; $P_{adj}=4.50x10^{-120}$) and *Card11* ($\log_2FC=-1.37$; $P_{adj}=3.92x10^{-12}$), but also upregulate *Ddx58* ($\log_2FC=1.75$; $P_{adj}=3.91x10^{-62}$) and *Trim25* ($\log_2FC=1.12$; $P_{adj}=2.22x10^{-40}$) in macrophages, which suggested that the N protein may start up signal transduction that leads to the production of IFN in response to viral infection, and it may even regulate apoptosis and survival of macrophages through the NF-κB signaling pathway.

Table VI. Signal transduction pathways of the N protein group.

KEGG ID	Description	Upregulated genes	Number of downregulated genes	P_{adj}
mmu04630	JAK-STAT signaling pathway	10	19	$1.14x10^{-5}$
mmu04668	TNF signaling pathway	4	21	$4.57x10^{-4}$
mmu04064	NF-κB signaling pathway	5	17	$1.26x10^{-3}$
mmu04010	MAPK signaling pathway	7	31	$1.12x10^{-2}$

KEGG, Kyoto Encyclopedia of Genes and Genomes; P_{adj}, adjusted P-value.

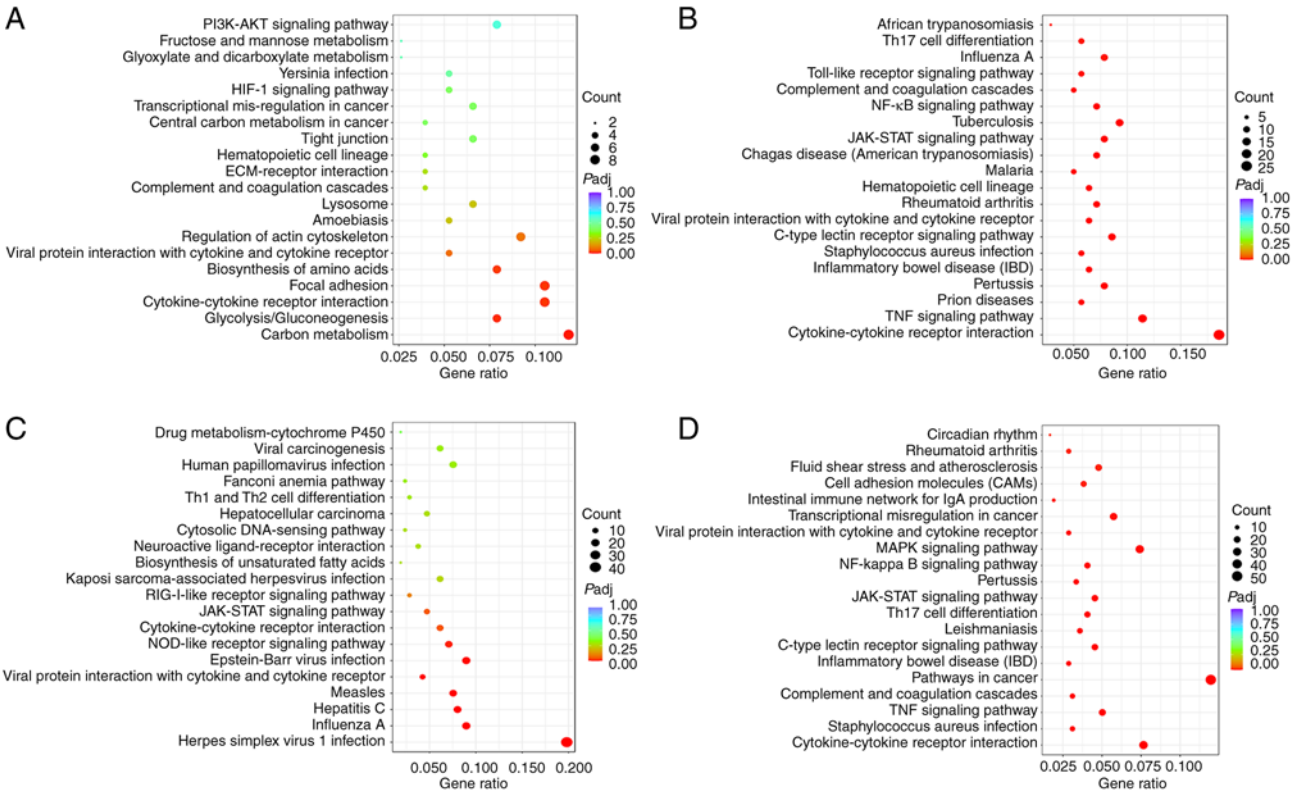

Figure 6. Top 20 pathways of DEGs in the different groups. (A) Upregulated and (B) downregulated DEGS in the ConA group compared with the control group. (C) Up- and (D) downregulated DEGs in the N protein group compared with the control group. Gene Ratio is the ratio of DEGs in a pathway to the number of all annotated genes in this pathway. Count indicates the number of DEGs annotated in the pathway, indicated by a dot; the larger the dot, the more DEGs are enriched. The color gradient indicates the adjusted P-value by the Benjamini-Hochberg false discovery rate method. Only pathways with P_{adj}<1.00 are shown. ConA, concanavalin A; DEGs, differentially expressed genes; N, nucleocapsid protein.

Discussion

Infection with SARS-CoV-2 could cause acute lung injury, and one of the most important causes is the dysregulation of the immune system (23). In the current study, the results of *in vitro* cell viability experiments showed that the SARS-CoV-2 N protein promoted Raji (a B cell line), Jurkat (a T cell line) and Raw264.7 (a macrophage cell line) cell viability, and cell cycle assay showed that N protein could increase the proportion of cells in G_2/M phase in the cell population.

Among the aforementioned three immune cells, macrophages are considered one of the first lines in the defense against pathogens and are an indispensable key participant in both innate and adaptive immunity (24). The present study showed that the N protein promoted macrophages to secrete inflammatory factors including TNF-α, IL-6 and IL-10. This was consistent with previous studies (23,25,26). TNF-α, an inflammatory cytokine produced by macrophages/monocytes during acute inflammation, is important for resistance to infection. Moreover, TNF-α could induce the production of IL-6 which serves an important role in the innate immune system response against SARS-CoV-2 (27). Higher levels of IL-6 and IL-10 were found to be associated with more severe cases of COVID-19 (28). In addition, a previous study revealed that IL-10 produced by macrophages inhibited the adjacent cells to differentiate into classically activated macrophages, thereby

Table VII. The Key genes enriched in the four pathway.

Gene	Log2FC	Padj	Description
Ddx58	1.75	$3.91x10^{-62}$	DEAD/H box helicase 58
STAT2	1.16	$5.67x10^{-13}$	Signal transducer and activator of transcription 2
Il12rb1	1.13	$1.68x10^{-3}$	Interleukin 12 receptor, beta 1
Trim25	1.12	$2.22x10^{-40}$	Tripartite motif-containing 25
STAT1	1.09	$4.62x10^{-11}$	Signal transducer and activator of transcription 1
Dusp4	-1.26	$8.76x10^{-28}$	Dual specificity phosphatase 4
Dusp10	-1.33	$1.08x10^{-4}$	Dual specificity phosphatase10
Card11	-1.37	$3.92x10^{-12}$	Caspase recruitment domain family, member 11
Dusp2	-1.42	$4.04x10^{-5}$	Dual specificity phosphatase2
Dusp16	-1.68	$9.40x10^{-43}$	Dual specificity phosphatase 16
Dusp1	-2.05	$3.20x10^{-118}$	Dual specificity phosphatase 1
Malt1	-2.25	$4.50x10^{-120}$	MALT1 paracaspase
Dusp5	-2.39	$5.81x10^{-110}$	Dual specificity phosphatase 5
Cxcl10	-2.63	$1.54x10^{-40}$	Chemokine (C-X-C motif) ligand 10
Cxcl2	-3.77	$4.38x10^{-204}$	Chemokine (C-X-C motif) ligand 2
Dusp8	-4.21	$8.22x10^{-16}$	Dual specificity phosphatase 8
Cxcl1	-5.89	$4.99x10^{-4}$	Chemokine (C-X-C motif) ligand 1

Table VIII. Key mutations of the nucleocapsid protein across the severe acute respiratory syndrome coronavirus 2 major variants of concern.

Variant	Deletions	Mutations
A (B.1.1.7)	None	D3L, R203K, G204R and S235F
B (B.1.351)	None	T205I
Γ (P.1)	None	P80R, R203K and G204R
Δ (B.1.617.2)	None	D63G, R203M and D377Y
O (BA.1)	Δ31E, Δ32R and Δ33S	P13L, R203K and G204R
O (BA.2)	Δ31E, Δ32R and Δ33S	P13L, R203K, G204R and S413R
O (BA.2.12.1)	Δ31E, Δ32R and Δ33S	P13L, R203K, G204R and S413R
O (BA.2.75)	Δ31E, Δ32R and Δ33S	P13L, R203K, G204R and S413R
O (BA.4)	Δ31E, Δ32R and Δ33S	P13L, P151S, R203K and G204R, S413R
O (BA.5)	Δ31E, Δ32R and Δ33S	P13L, R203K, G204R and S413R
O (BQ.1.1)	Δ31E, Δ32R and Δ33S	P13L, E136D, R203K, G204R and S413R
O (XBB.1.5)	Δ31E, Δ32R and Δ33S	P13L, R203K, G204R and S413R

allowing the macrophage population to self-regulate (29). This suggested that the SARS-CoV-2 N protein may regulate the proportion of macrophages of the M1/M2 type in the macrophage population.

Consistent with the aforementioned findings, transcriptome analysis showed that the N protein could upregulate *spp1* (log_2FC=1.30; $P_{adj}=5.04x10^{-72}$) (19) and *Nos2* gene (log_2FC, 9.01; $P_{adj}=2.64x10^{-12}$) (30), which also meant that the N protein may promote microphages to secrete inflammatory cytokines and some of them may act on macrophages to adjust their ability to function in immune defense. Moreover, the GO enrichment analysis showed that DEGs of the N group were significantly enriched in the inflammatory response, positively regulating cytokine production and other immune defense responses such as response to 'interferon-beta' and 'leukocyte differentiation'. These findings showed that the N protein may regulate host immunity, which is in line with previous studies (10,12).

The goal of signal transduction is to find the response that optimally safeguards survival (31). KEGG analysis showed that the N protein is likely to achieve its role by accurately regulating the JAK-STAT, TNF, NF-κB and MAPK signaling pathways. Although a number of studies have confirmed relatively low variability of SARS-CoV-2 genomes, there are still more variants than expected owing to the high transmission rates and the large number of infected individuals in the pandemic (8,32). The transmission speed, infection efficiency and clinical manifestations caused by these variants are different (33). A number of previous studies have shown that

the adaptive mutations of the S protein contributed to the spread and virulence of the virus (34,35). In addition to the mutations of the S protein, mutations in the N protein are also important for viral spread during the pandemic (36,37). The SARS-CoV-2 N protein expressed in the present study came from wild-type Wuhan-1 and comprised two RNA-binding domains, the N-and the C-terminal domains, and three intrinsically disordered regions (IDRs), IDR1-IDR3 (38-40). Compared with the wild-type, the N protein was mutated in several strains of variants of concern (Table VIII) (41,42). In the current study, three types of immune cells, Raw264.7, Jurkat and Raji, were selected as model cells to investigate the immune activity of the three types of immune cells and possible molecular mechanisms of the N protein on Raw264.7 cells. These cells are not identical to primary cells found in living organisms and may not perfectly represent the behavior of primary cells found in organisms. However, given the commonalities between model cells and primary cells, the current study could provide a theoretical basis for the immune regulatory activity and molecular mechanism of N protein at the cellular and molecular levels. B-cell-linear epitopes and T-cell epitopes of the N protein are conserved in the main SARS-CoV-2 variants including A (B.1.1.7), O (BA.1), O (XBB.1.5) (43-47), which means that the results of the current study may have similarities with *in vitro* immunomodulatory activity of the conserved N protein of the major variant strains of SARS-CoV-2. In addition, the findings that N protein has regulatory activity on RAW264.7, Jurkat and Raji, and can affect the expression of genes in innate immunity and acquired immunity supported the vaccination strategies designed to target the N protein that could generate immune responses which had cross-reactivity with SARS-CoV-2, as well as the potential ability to protect or modulate disease. The present study may also support new medical strategies developed to targeting the SARS-CoV-2 N protein, which may moderately alleviate immune system disorders such as excessive secretion of cytokines which may cause cytokine storm after infection by SARS-CoV-2. The present study has certain limitations. Raw264.7, Jurkat and Raji cells were selected as model cells which are not identical to primary cells found in living organisms and may not represent the behavior of primary cells found in organisms. In future research, the *in vitro* and *in vivo* immune response activity of the N protein in primary cells will be further explored. In conclusion, the current study provided a hypothesis for how the N-protein may regulate gene expression changes in macrophages in innate immunity after it enters the body and the mechanism of the N protein participating in innate and adaptive immunity.

Acknowledgements

Not applicable.

Funding

The present study was supported by The Sichuan Province Science and Technology Support Project (grant nos. 2022NSFSC0107, 2022NZZJ0003 and 22ZYZFSF0009), The Nanchong City Science and Technology Project (grant nos. 20YFZJ0053 and 20YFZJ0054), and The Open Project of Sichuan Provincial Key Laboratory of Central Nervous System Drugs (grant no. 210023-01SZ).

Availability of data and materials

The datasets used and/or analyzed during the current study are available from the corresponding author on reasonable request. The transcriptome data have been uploaded to the Gene Expression Omnibus database (accession no. GSE236800).

Authors' contributions

YH and XD conceived and designed the experiments of the present study. YL, ZY, XL, XD and YH performed the experiments and acquired the data. YL, ZY, XL, LZ, XD and YH confirm the authenticity of all the raw data. YL, LZ and YH drafted the manuscript and revised it critically. All authors read and approved the final manuscript.

Ethics approval and consent to participate

Not applicable.

Patient consent for publication

Not applicable.

Competing interests

The authors declare that they have no competing interests.

References

1. Han Q, Lin Q, Jin S and You L: Coronavirus 2019-nCoV: A brief perspective from the front line. J Infect 80: 373-377, 2020.
2. Deng SQ and Peng HJ: Characteristics of and public health responses to the coronavirus disease 2019 outbreak in China. J Clin Med 9: 575, 2020.
3. Coronaviridae Study Group of the International Committee on Taxonomy of Viruses: The species severe acute respiratory syndrome-related coronavirus: Classifying 2019-nCoV and naming it SARS-CoV-2. Nat Microbiol 5: 536-544, 2020.
4. Zhu N, Zhang D, Wang W, Li X, Yang B, Song J, Zhao X, Huang B, Shi W, Lu R, *et al*: A Novel coronavirus from patients with pneumonia in China, 2019. N Engl J Med 382: 727-733, 2020.
5. Wu F, Zhao S, Yu B, Chen YM, Wang W, Song ZG, Hu Y, Tao ZW, Tian JH, Pei YY, *et al*: A new coronavirus associated with human respiratory disease in China. Nature 579: 265-269, 2020.
6. Zhou P, Yang XL, Wang XG, Hu B, Zhang L, Zhang W, Si HR, Zhu Y, Li B, Huang CL, *et al*: A pneumonia outbreak associated with a new coronavirus of probable bat origin. Nature 579: 270-273, 2020.
7. Chan JF, Kok KH, Zhu Z, Chu H, To KK, Yuan S and Yuen KY: Genomic characterization of the 2019 novel human-pathogenic coronavirus isolated from a patient with atypical pneumonia after visiting Wuhan. Emerg Microbes Infect 9: 221-236, 2020.
8. Lu R, Zhao X, Li J, Niu P, Yang B, Wu H, Wang W, Song H, Huang B, Zhu N, *et al*: Genomic characterisation and epidemiology of 2019 novel coronavirus: Implications for virus origins and receptor binding. Lancet 395: 565-574, 2020.
9. Masters PS and Sturman LS: Background paper. Functions of the coronavirus nucleocapsid protein. Adv Exp Med Biol 276: 235-238, 1990.
10. Mu J, Xu J, Zhang L, Shu T, Wu D, Huang M, Ren Y, Li X, Geng Q, Xu Y, *et al*: SARS-CoV-2-encoded nucleocapsid protein acts as a viral suppressor of RNA interference in cells. Sci China Life Sci 63: 1413-1416, 2020.

11. Chen K, Xiao F, Hu D, Ge W, Tian M, Wang W, Pan P, Wu K and Wu J: SARS-CoV-2 nucleocapsid protein interacts with RIG-I and represses RIG-mediated IFN-β production. Viruses 13: 47, 2020.
12. Mu J, Fang Y, Yang Q, Shu T, Wang A, Huang M, Jin L, Deng F, Qiu Y and Zhou X: SARS-CoV-2 N protein antagonizes type I interferon signaling by suppressing phosphorylation and nuclear translocation of STAT1 and STAT2. Cell Discov 6: 65, 2020.
13. Netea MG, Schlitzer A, Placek K, Joosten LAB and Schultze JL: Innate and adaptive immune memory: An evolutionary continuum in the host's response to pathogens. Cell Host Microbe 25: 13-26, 2019.
14. Ding SW, Han Q, Wang J and Li WX: Antiviral RNA interference in mammals. Curr Opin Immunol 54: 109-114, 2018.
15. Sadler AJ and Williams BRG: Interferon-inducible antiviral effectors. Nat Rev Immunol 8: 559-568, 2008.
16. Mick DU, Fox TD and Rehling P: Inventory control: Cytochrome c oxidase assembly regulates mitochondrial translation. Nat Rev Mol Cell Biol 12: 14-20, 2011.
17. Dudkina NV, Kouril R, Peters K, Braun HP and Boekema EJ: Structure and function of mitochondrial supercomplexes. Biochim Biophys Acta 1797: 664-670, 2010.
18. Acín-Pérez R, Bayona-Bafaluy MP, Fernández-Silva P, Moreno-Loshuertos R, Pérez-Martos A, Bruno C, Moraes CT and Enríquez JA: Respiratory complex III is required to maintain complex I in mammalian mitochondria. Mol Cell 13: 805-815, 2004.
19. Lamort AS, Giopanou I, Psallidas I and Stathopoulos GT: Osteopontin as a link between inflammation and cancer: The thorax in the spotlight. Cells 8: 815, 2019.
20. Saheb Sharif-Askari F, Saheb Sharif-Askari N, Goel S, Hafezi S, Assiri R, Al-Muhsen S, Hamid Q and Halwani R: SARS-CoV-2 attenuates corticosteroid sensitivity by suppressing DUSP1 expression and activating p38 MAPK pathway. Eur J Pharmacol 908: 174374, 2021.
21. Goel S, Saheb Sharif-Askari F, Saheb Sharif Askari N, Madkhana B, Alwaa AM, Mahboub B, Zakeri AM, Ratemi E, Hamoudi R, Hamid Q and Halwani R: SARS-CoV-2 switches 'on' MAPK and NFκB signaling via the reduction of nuclear DUSP1 and DUSP5 expression. Front Pharmacol 12: 631879, 2021.
22. Tripathy AS, Vishwakarma S, Trimbake D, Gurav YK, Potdar VA, Mokashi ND, Patsute SD, Kaushal H, Choudhary ML, Tilekar BN, *et al*: Pro-inflammatory CXCL-10, TNF-α, IL-1β, and IL-6: Biomarkers of SARS-CoV-2 infection. Arch Virol 166: 3301-3310, 2021.
23. Polidoro RB, Hagan RS, de Santis Santiago R and Schmidt NW: Overview: Systemic inflammatory response derived from lung injury caused by SARS-CoV-2 infection explains severe outcomes in COVID-19. Front Immunol 11: 1626, 2020.
24. Atri C, Guerfali FZ and Laouini D: Role of human macrophage polarization in inflammation during infectious diseases. Int J Mol Sci 19: 1801, 2018.
25. Huang C, Wang Y, Li X, Ren L, Zhao J, Hu Y, Zhang L, Fan G, Xu J, Gu X, *et al*: Clinical features of patients infected with 2019 novel coronavirus in Wuhan, China. Lancet 395: 497-506, 2020.
26. Chen G, Wu D, Guo W, Cao Y, Huang D, Wang H, Wang T, Zhang X, Chen H, Yu H, *et al*: Clinical and immunological features of severe and moderate coronavirus disease 2019. J Clin Invest 130: 2620-2629, 2020.
27. Abdin SM, Elgendy SM, Alyammahi SK, Alhamad DW and Omar HA: Tackling the cytokine storm in COVID-19, challenges and hopes. Life Sci 257: 118054, 2020.
28. Han H, Ma Q, Li C, Liu R, Zhao L, Wang W, Zhang P, Liu X, Gao G, Liu F, *et al*: Profiling serum cytokines in COVID-19 patients reveals IL-6 and IL-10 are disease severity predictors. Emerg Microbes Infect 9: 1123-1130, 2020.
29. Katakura T, Miyazaki M, Kobayashi M, Herndon DN and Suzuki F: CCL17 and IL-10 as effectors that enable alternatively activated macrophages to inhibit the generation of classically activated macrophages. J Immunol 172: 1407-1413, 2004.
30. Vuolteenaho K, Koskinen A, Kukkonen M, Nieminen R, Päivärinta U, Moilanen T and Moilanen E: Leptin enhances synthesis of proinflammatory mediators in human osteoarthritic cartilage-mediator role of NO in leptin-induced PGE2, IL-6, and IL-8 production. Mediators Inflamm 2009: 345838, 2009.
31. Marks F, Klingmüller U and Müller-Decker K: Cellular signal processing: An introduction to the molecular mechanisms of signal transduction. 2nd edition. Garland Science, 2017.
32. Ceraolo C and Giorgi FM: Genomic variance of the 2019-nCoV coronavirus. J Med Virol 92: 522-528, 2020.
33. Cojocaru C, Cojocaru E, Turcanu AM and Zaharia DC: Clinical challenges of SARS-CoV-2 variants (Review). Exp Ther Med 23: 416, 2022.
34. Flores-Vega VR, Monroy-Molina JV, Jiménez-Hernández LE, Torres AG, Santos-Preciado JI and Rosales-Reyes R: SARS-CoV-2: Evolution and emergence of new viral variants. Viruses 14: 653, 2022.
35. Scovino AM, Dahab EC, Vieira GF, Freire-de-Lima L, Freire-de-Lima CG and Morrot A: SARS-CoV-2's variants of concern: A brief characterization. Front Immunol 13: 834098, 2022.
36. Yun JS, Song H, Kim NH, Cha SY, Hwang KH, Lee JE, Jeong CH, Song SH, Kim S, Cho ES, *et al*: Glycogen synthase kinase-3 interaction domain enhances phosphorylation of SARS-CoV-2 nucleocapsid protein. Mol Cells 45: 911-922, 2022.
37. Wu H, Xing N, Meng K, Fu B, Xue W, Dong P, Tang W, Xiao Y, Liu G, Luo H, *et al*: Nucleocapsid mutations R203K/G204R increase the infectivity, fitness, and virulence of SARS-CoV-2. Cell Host Microbe 29: 1788-1801.e6, 2021.
38. Dinesh DC, Chalupska D, Silhan J, Koutna E, Nencka R, Veverka V and Boura E: Structural basis of RNA recognition by the SARS-CoV-2 nucleocapsid phosphoprotein. PLoS Pathog 16: e1009100, 2020.
39. Bai Z, Cao Y, Liu W and Li J: The SARS-CoV-2 nucleocapsid protein and its role in viral structure, biological functions, and a potential target for drug or vaccine mitigation. Viruses 13: 1115, 2021.
40. Carlson CR, Asfaha JB, Ghent CM, Howard CJ, Hartooni N, Safari M, Frankel AD and Morgan DO: Phosphoregulation of phase separation by the SARS-CoV-2 N protein suggests a biophysical basis for its dual functions. Mol Cell 80: 1092-1103.e4, 2020.
41. Liang F: Quantitative mutation analysis of genes and proteins of major SARS-CoV-2 variants of concern and interest. Viruses 15: 1193, 2023.
42. Hossain A, Akter S, Rashid AA, Khair S and Alam ASMRU: Unique mutations in SARS-CoV-2 Omicron subvariants' non-spike proteins: Potential impacts on viral pathogenesis and host immune evasion. Microb Pathog 170: 105699, 2022.
43. Rodrigues-da-Silva RN, Conte FP, da Silva G, Carneiro-Alencar AL, Gomes PR, Kuriyama SN, Neto AAF and Lima-Junior JC: Identification of B-cell linear epitopes in the nucleocapsid (N) protein B-cell linear epitopes conserved among the main SARS-CoV-2 variants. Viruses 15: 923, 2023.
44. Lee E, Sandgren K, Duette G, Stylianou VV, Khanna R, Eden JS, Blyth E, Gottlieb D, Cunningham AL and Palmer S: Identification of SARS-CoV-2 nucleocapsid and spike T-cell epitopes for assessing T-cell immunity. J Virol 95: e02002-20, 2021.
45. Oliveira SC, de Magalhães MTQ and Homan EJ: Immunoinformatic analysis of SARS-CoV-2 nucleocapsid protein and identification of COVID-19 vaccine targets. Front Immunol 11: 587615, 2020.
46. Verhagen J, van der Meijden ED, Lang V, Kremer AE, Völkl S, Mackensen A, Aigner M and Kremer AN: Human $CD4^+$ T cells specific for dominant epitopes of SARS-CoV-2 Spike and Nucleocapsid proteins with therapeutic potential. Clin Exp Immunol 205: 363-378, 2021.
47. Pacheco-Olvera DL, Saint Remy-Hernández S, García-Valeriano MG, Rivera-Hernández T and López-Macías C: Bioinformatic analysis of B- and T-cell epitopes from SARS-CoV-2 structural proteins and their potential cross-reactivity with emerging variants and other human coronaviruses. Arch Med Res 53: 694-710, 2022.